

A Microfluidic Particle-analyzing Device with Novel Coplanar Electrode Design Based on Impedance Sensing

Chia-Hong Gao, Ting-Wei Wu and Chih-Ting Lin

Graduate Institute of Electronics Engineering, National Taiwan University, Taipei 10617, Taiwan (R.O.C.)

r04943173@ntu.edu.tw; r03943068@ntu.edu.tw; timlin@ntu.edu.tw

Abstract— Single cell detection is an important technology in cellular and molecular biology, immunology and physiology. Recently, the develop of flow cytometry provide a convenient, fast and accurate way to do single cell detection. The most common detection way used in flow cytometry is optical method. However, although this kind of optical method is accurate, the equipment is bulky, and the operators should be well trained. These disadvantages are the constraints when we want to develop a portable device. Therefore, flow cytometry with impedance sensing is proposed. It is small in size, convenient, and low cost, so it has the potential to develop as a portable device. This research use photo-lithography to fabricate electrodes in several tens of micro meter and PDMS microfluidic channel to discuss the properties and capabilities of flow cytometry with impedance sensing used co-planar electrodes, including electrode dimension effect and the height of sensing target effect. In addition, a series of experiment is done to demonstrate the capabilities of size and location discrimination of particle with 3 μm , 6 μm and 10 μm in diameter. The electrode scale in this thesis is also discussed for its influence on the sensing ability.

Keywords—Microfluidics; Impedance; Flow Cytometry; Particle Analysis

I. INTRODUCTION

Nowadays, bio-particle detection and analyzing play an important role in daily life. By analyzing bio-material and bio-particle, such as bacteria, virus, antibody, specific biomarker, circular tumor cells...etc, we can know many information related to the sensing target [1-3]. For single cell analysis, optical flow cytometer provides a precise cell information collection by analyzing receptive data of lights reflected on cells [4-5]. However, it is mostly restricted to its bulky size, high cost and extra expense on labeling. Therefore, impedance flow cytometry is proposed to fulfill the need of a portable single cell analysis device [6-7]. Such that Renaud et al proposed the first microfluidics-based impedance cytometer by differentiating beads of 5 μm and 8 μm at 1.72MHz [7].

Different from parallel electrode design suffering from complex fabrication on alignment [6], coplanar electrodes are then newly spatial-designed to achieve an easier fabrication procedure and mitigate non-uniform electric field by squeezing the channel height [8]. By pumping polystyrene beads with different sizes into the channel, information about size and position could be obtained by the aid of two reference sensing electrodes. Different sizes of electrode width could be demonstrated to affect signal variance from detection of a lock-in amplifier. The device then shows successful ability of differentiating these beads with different properties.

II. EXPERIMENT

A. Fabrication Process

The fabrication procedure could be shown in the previous work [8]. To elaborate on, there are two parts both fabricated in the clean room: the sensing electrode and microfluidics channel mode which are shown in Fig. 1. Glass slide was used as the substrate, and positive photoresist (s1813) was spin-coated on it with 4000 rpm. Photolithography and developing define the electrode pattern first. Glass substrate with defined photoresist residue will be then evaporated by 20 nm chromium and 50 nm gold and lifted off to produce the electrode-defined substrate. In the other part, silicon wafer will be spin-coated on SU8 2005 photoresist with 410 rpm to create a rough 11 μm thickness. After the second lithography defines the microchannel pattern, the polydimethylsiloxane (PDMS) will be poured on this mold and peeled off to have the channel. Afterwards, it will be bounded to the mentioned oxygen-plasma treated glass substrate with the planar electrodes. The composite will be finally placed on a printed circuit board (PCB) so that the electrical signal can be applied onto and measured from the electrodes. The real picture of sensing device is shown in Fig. 2.

B. Device Design and Parameters

To obtain particle size and position information, the schematic of electrode dimension and shape design could be shown in Fig. 3. 4 electrodes with 20 μm width and gap are measured as across (A-C) and neighbor (A-B) signal, where 1V ac signal is applied on A and output signal is returned back to a lock-in amplifier from B or C. As follows, three position differentiation regions, i.e. far, center, near regions, of bead position are shown too in Fig. 3a. As for the microfluidics channel, its schematic could be shown in Fig. 3b. The dimension is designed as 60 μm in width and the channel height is 11 μm in order to suppress the fluorescent beads to the surface of electrode. Other than the schematics, fluorescent beads of 10 μm , 6 μm and 3 μm are utilized to demonstrate the sensing ability of electrodes. Their sizes are according to the cell size in human body due to the final aim of applying on the detection of circular tumor cell (CTC). 1% pluronic is further used to deal with modifying the surface property of beads from hydrophobic to hydrophilic. Moreover, 300mM Potassium Chloride (KCL) solution is used as buffer where the concentration provides an adequate conductivity of 1.7 S/m in impedance sensing. Signal responses under different ion concentration could be shown in Fig. 4. Eventually, frequency around 1MHz is chosen to be the operational frequency in this device in reference to the work of Renaud et al. in 2001 [7].

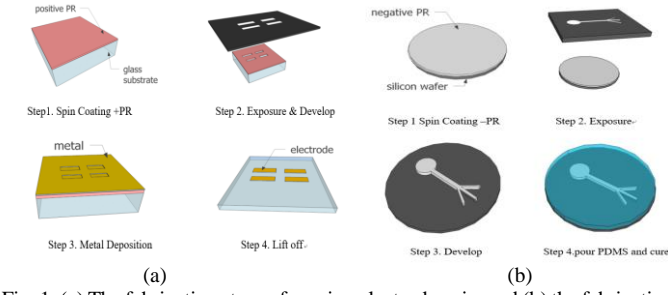


Fig. 1. (a) The fabrication steps of sensing electrode pairs and (b) the fabrication steps of microchannel mode.

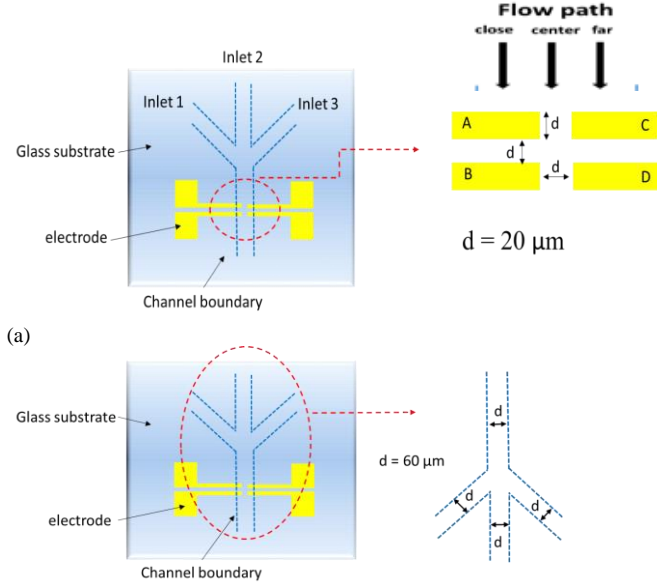


Fig. 2. (a) The schematic of sensing electrode and (b) microchannel design where scale of electrodes and different flow path are specified.

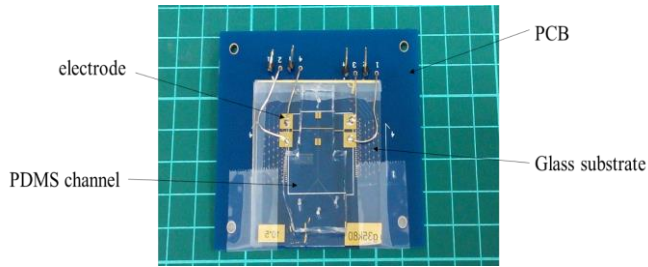


Fig. 3. The real picture of sensing device.

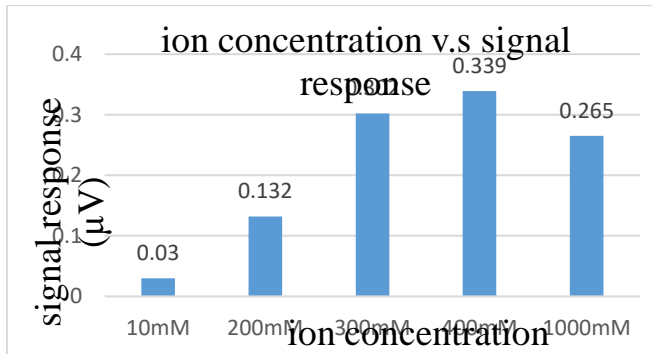


Fig. 4. The signal responses under different ion concentration of KCL.

III. RESULT AND DISCUSSION

A. Bead Height Effect

Due to the characteristics that all the electrodes are on the same plane, non-uniform electrical field is built. The region near the surface of electrode is with stronger electric field than the region far away from the electrode. As shown in Fig. 5, the electrical potential (color distribution) and electrical field (arrows) was simulated by simulation tool, COMSOL. In this simulation, channel height of $25 \mu\text{m}$ is considered, and then, one volt was applied on the bottom of left hand side, while potential of the other side was zero volt. We can notice that the potential distribution was decrease as height increasing.

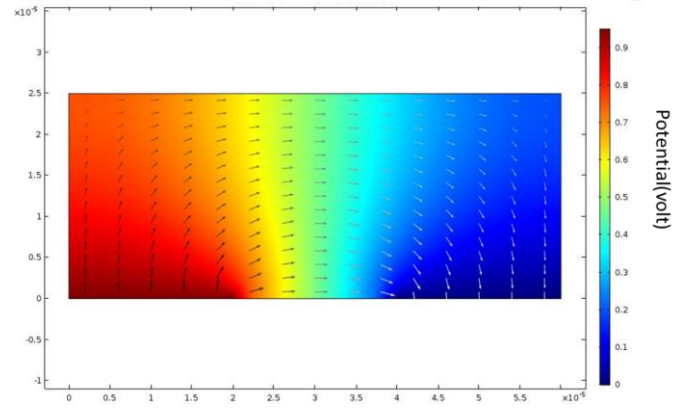


Fig. 5. Simulation of potential distribution by COMSOL.

Hence, the height of beads should be taken into account when conducting the impedance sensing. There are two factors that have influence on the bead height. One is the channel height of microfluidics channel which has already been determined during the fabrication process. The other is the flow rate of KCL solution. For the first factor, channel height of microfluidics channel, if the channel height is high, the beads have the chance to distribute among the high position which mean far away from the surface of electrode, leading to a small signal response when beads passing through the sensing area. Microfluidics channel with $50 \mu\text{m}$ height had ever been tried to measure the signal response, however, no signal response was detected when some beads did pass though the sensing area. Similarly, $25 \mu\text{m}$ height microfluidics channel is also not suitable for impedance sensing. Finally, $11 \mu\text{m}$ channel height is proved to be capable of sensing the signal response of beads with $3 \mu\text{m}$, $6 \mu\text{m}$, $10 \mu\text{m}$ in diameter. For the other factor that affect the bead height, flow rate of KCL solution, the reason is the velocity gradient induced hydrodynamic force.

Due to the velocity difference between different position, a force induced by the velocity gradient will happen on the particle in the channel. The direction of this force point to middle height of the channel which is the place with highest flow velocity. Thus, the faster the flow rate is, the closer the position of beads is to the middle height of channel. In other word, flow rate plays a role on the height of beads. The research results of Renaud et al [7] also show the characteristics of bead height effect as shown in Fig. 6. We can make a conclusion that the faster the flow rate is, the smaller the signal response is. Based on the hypothesis, we further insert beads into microchannel by varying

their flow rates to see the relationship between them and the proceeding signal responses in Fig. 6.

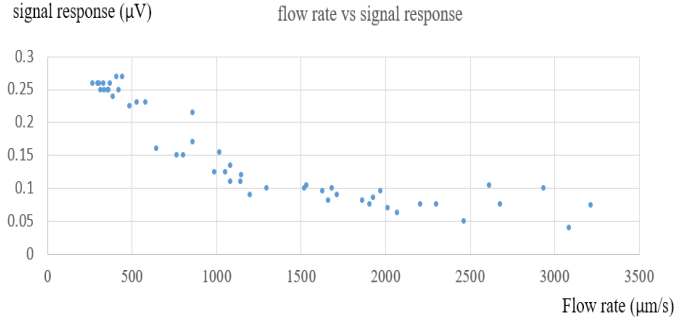


Fig. 6. The bead height effect of flow rate and signal response.

By the experiment results, we can find that bead height is an important factor that affect signal response very much. Comparing the signal response at 500 $\mu\text{m/s}$ and 2500 $\mu\text{m/s}$, the one of 500 $\mu\text{m/s}$ is about 5 times larger than the one at 2500 $\mu\text{m/s}$. However, the bead height effect is the characteristic that we don't want due to the influence on sensing accuracy. Thus, in order to conquer this problem, microfluidics channel height was reduced down to 11 μm and the flow rate should not vary too much. In this experiment, flow rate is controlled within the range from 400 $\mu\text{m/s}$ to 500 $\mu\text{m/s}$.

B. Bead Size and Position Effect

In this sub-section, the sensing abilities of bead position and size are demonstrated here by using beads of 3 μm , 6 μm , 10 μm . As illustrated in the section of experiment method, two electrical signals were measured, which are Across signal and Neighbor signal. These two signal are plotted as the x-axis and y-axis in the experiment results as shown in Fig. 7. The dash-line ellipse in Fig. 7 was made by using the 2 times standard deviation of Across signal as the ellipse major axis, while 2 times standard deviation of Neighbor signal was used as the ellipse minor axis. In Fig. 7a, the signal response of far side is zero, which means the electrode cannot sense the event of passing through of 3 μm beads on far path. There are two reasons for this phenomenon. First, the size of 3 μm beads is too small which cannot cause a significant interfere of electrical field. In other word, the interfere to the electrical field of 3 μm bead on far path is at the same level as background noise. Second, the flow path is far away from the position that the electrical field strength changes most dramatically. The more dramatically the electrical field strength change, the more sensitive the electrode is to the event of beads passing through. For the other two paths, center side and close side, there are signal responses of Neighbor signal only on close path, while the signal of Across only response on the center way. By the experiment results in Fig. 7a, it indicates the most sensitive positon of each electrode. The most sensitive position of Neighbor signal is close path, and is center path for Across signal. Hence, by the distribution of signal response in Fig. 7, we can know the flow path of beads, which is called the position effect.

On the other hand, bead size effect can be observed by comparing the three charts in Fig. 7. In the results of 6 μm beads, comparing to the results of 3 μm beads, we can notice that the signal response of flowing on close path can not only be detected

by the Neighbor signal but also Across signal. Similarly, the beads on center side also can be detected by both signal. The most different is the that beads of 6 μm can be detected by at least one signal. Furthermore, we can find the 10 μm beads are the one that can be detected most easily. All three paths of 10 μm beads can be detected by both signal. In addition to the signals, Neighbor or Across, that can detect the bead in different flow path, the signal response also increase as the bead size increase. Thus, by comparing three charts of Fig. 7, we can observe the bead size effect.

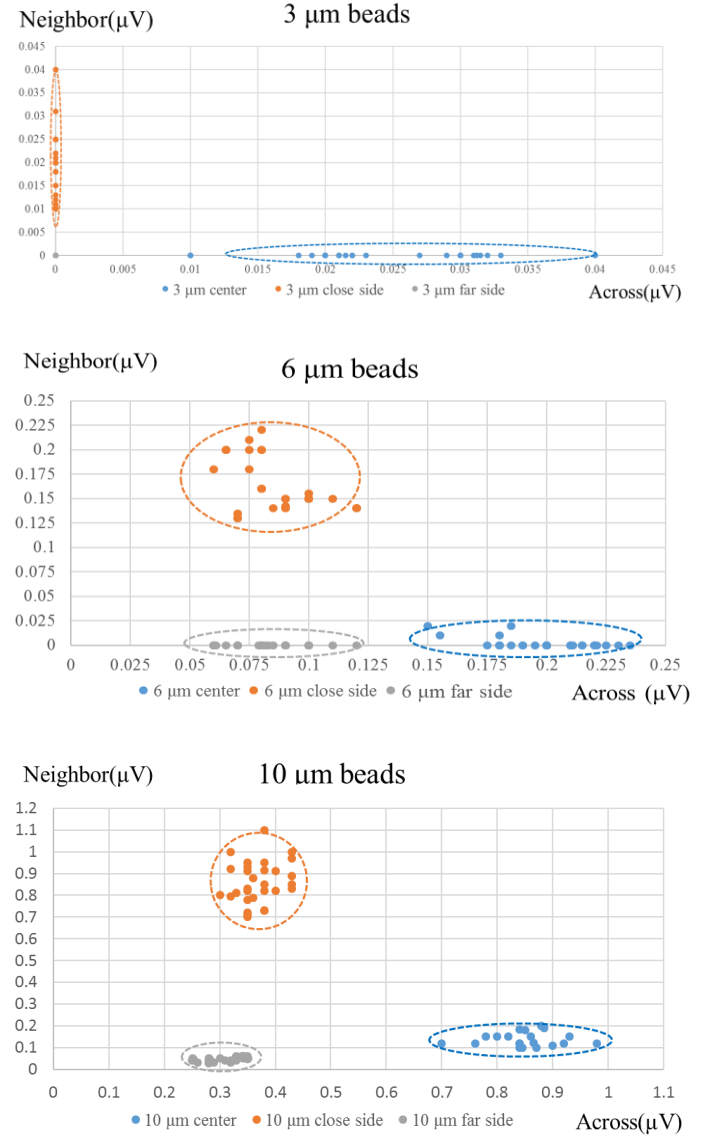


Fig. 7 Signal responses of beads with different sizes: 3, 6 and 10 μm from up to down.

In order to demonstrate the ability to distinguish beads with unknown size and unknown flow path, three experiment results charts are merged into one chart as shown in Fig. 8. By this chart, we can find that there is no overlap between any two data group. Hence, we can say that this set of sensing electrode is capable of tell the unknown bead size and unknown position simultaneously. Furthermore, the experiment results do not very fit the Coulter Principle which state that the signal response

amplitude is proportional to the bead size since our electrode design is coplanar that induce a non-uniform electrical field while the Coulter Principle is based on uniform electrical field. However, even though my experiments were conduct under non uniform electrical field, there are still good positive relationship between bead size and signal response amplitude. In other word, as the bead size increase a lot, the signal responses also increase a lot. If the bead size just increases a little, the signal responses will not increase too much.

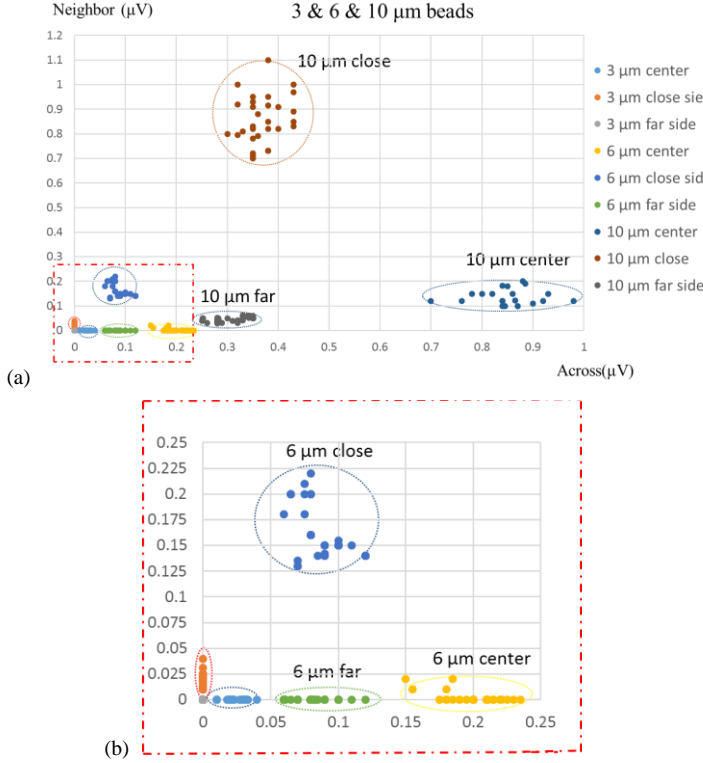


Fig. 8. (a) The signal responses for three kinds of beads on different three flow paths and (b) the close look of a specified region.

C. Area of Sensing Region Effect

The area of the sensing region is also interesting to us since different scale of electrode will also affect sensitivity. Hence, a series of experiment was done to compare the area of sensing region to see if this really occurs. In this experiment, two kinds of design dimension were used to compare the area of sensing effect. One is the dimension with $d = 10 \mu\text{m}$, and the other is the dimension with $d = 20 \mu\text{m}$. The major difference between this two design dimensions is that the electrical field strength between electrodes. So, the electrical signal change when beads pass through must be different between this two cases.

The experiment results were shown in Fig. 9. In this series of experiment, fluorescent beads of $3 \mu\text{m}$ and $6 \mu\text{m}$ were used. In Fig. 9a, the area of sensing region effect on $3 \mu\text{m}$ beads were shown. It can be noticed that the signal responses are different between two electrode design dimension. The signal responses of Neighbor signal measured by sensing design with $d=10 \mu\text{m}$ are larger than the ones measured by $d=20 \mu\text{m}$. Because the electrical field in the case of $d = 10 \mu\text{m}$ is stronger than the case of $d=20 \mu\text{m}$, the disturbance of electrical signal caused by a

passing bead would be more significant. However, we can also notice that the signal responses of Across signals are not significantly different in both case. Since the electrical field is non uniform along the direction of height, the dielectrophoresis (DEP) phenomenon should be taken into account. Dielectrophoresis force is a force caused by non-uniform electrical field and the magnitude of dielectrophoresis force are proportional to the volume of beads and also the strength of electrical field gradient. Due to dielectrophoresis force, the beads will be lift up when passing through sensing region. Thus, the beads will locate at the height where the electrical field is weaker than the original height, leading to a smaller signal response. So, the signal responses are not significant different between two electrode design dimension. Nevertheless, dielectrophoresis force have an influence on the both Neighbor and Across signal, we can only obtain different signal response magnitude on close flow pass because the bead height is closer to the surface when passing through close path than passing through center path. In other word, even though bead was lift up by DEP force in the case of flowing through close path, the electrical signal strength is still strong enough leading the difference signal response in Neighbor signal.

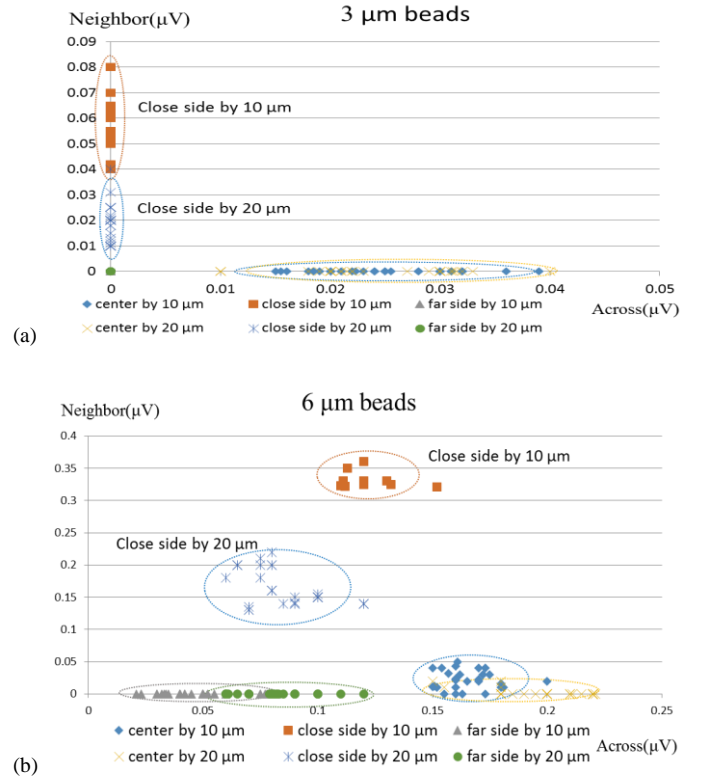


Fig. 9. The area of sensing electrode effect of (a) $3 \mu\text{m}$ and (b) $6 \mu\text{m}$ beads.

IV. CONCLUSIONS

A novel electrode design was proposed and verified to be capable of detecting the beads size and position. Beads of $3 \mu\text{m}$, $6 \mu\text{m}$, and $10 \mu\text{m}$ can be successfully distinguished on any one of the three flow path. However, there is one disadvantage of this sensing device. That is the channel height. The channel height in my experiment is $11 \mu\text{m}$. The major reason for the low

channel is only under such low channel, signal response of beads of 3 μm can be measured. However, such low channel height will induce some problems in practical use. For example, if the sample under detection is blood, we need sample preparation process to fill out the particles or defects larger than 11 μm , or the channel will be stuck. Instead of reducing the channel height, a top-down hydrodynamic focusing skill is also a choice to keep the beads close to the electrode surface. However, due to the using of top-down focusing flow stream, to some extent, it will reduce the simplicity of use.

In the future, the top-down hydrodynamic focus skill will be tied and another novel electrode with non-symmetry spatial design will be proposed to detect the property of cell, such as resistance of cytoplasm. The position and size information will be taken as a reference information to correct or calibrate the sensing results of back-end sensors.

ACKNOWLEDGMENT

The authors are grateful to NTU Nano-BioMEMS Group and NTU CMOS Biotechnology LAB. All microfabrication was done in NTU Graduate Institute of Electronics Engineering.

REFERENCES

- [1] Pei-Wen Yen and Yen-Pei et al, "LuEmerging Electrical Biosensors for Detecting Pathogens and Antimicrobial Susceptibility Tests" *Current organic chemistry*, 18, 165-172, 2014.
- [2] Fei Liu and Anis Nurashikin Nordin et al, "A lab-on-chip cell-based biosensor for label-free sensing of water toxicants", *Lab on a Chip*, 14, 1270, 2014.
- [3] Grace M. Credo and Xing Su et al, "Label-free electrical detection of pyrophosphate generated from DNA polymerase reactions on field-effect devices", *Analyst*, 137, 1343-1350, 2012.
- [4] Valery V. Tuchin, "Advanced Optical Flow Cytometry: Methods and Disease Diagnoses," Wiley-VCH, ISBN 978-3-527-40934-1, 2011.
- [5] A Tzur et al, "Optimizing Optical Flow Cytometry for Cell Volume-Based Sorting and Analysis," *PLoS ONE*, Vol 6, Jan, 2011.
- [6] H. E. Ayliffe, A. B. Frazier and R. D. Rabbit, "Electric impedance spectroscopy using microchannels with integrated metal electrodes," *J Microelectromech Syst*, 8, 50-57.
- [7] S. Gawad, L. Schild and Ph. Renaud, "Micromachined impedance spectroscopy flow cytometer for cell analysis and particle sizing," *Lab Chip*, 1, 76-82, 2001.
- [8] T.-W. Wu, C.-H. Kao, and C.-T. Lin, "A Microfluidic Cell Counting Device Based on Impedance Analysis," 16th International Meeting on Chemical Sensors, Jeju, Korea, Jul. 2016.